

The 3 μm spectra of candidate carbon stars^{*}

M.A.T. Groenewegen^{1,2}, T. de Jong^{1,3}, and T. R. Geballe⁴

¹ Astronomical Institute, Kruislaan 403, NL-1098 SJ Amsterdam, The Netherlands

² present address: Institut d'Astrophysique de Paris, 98bis Bld. Arago, F-75014 Paris, France

³ Space Research Groningen, P.O. Box 800, NL-9700 AV Groningen, The Netherlands

⁴ Joint Astronomy Centre, 660 N. A'ohoku Place, University Park, Hilo, HI 96720, USA

Received 25 November 1993 / Accepted 25 January 1994

Abstract. We have searched for the 3.1 μm absorption feature, a well-known characteristic of optical carbon stars, in a sample of sixteen candidate carbon stars, most of which have very red colors and some of which have no optical counterparts. The sample was selected on the basis of similarity of LRS spectra to those of known carbon stars. We detected the 3.1 μm feature in eleven candidates, confirming them as carbon stars. There is a wide range in the strength of the feature. In general, the 3.1 μm feature weakens with redder $[K - L]$ color. However, two of the reddest stars (with $[K - L] = 5$) show the strongest features. Models of the spectrum near the 3.1 μm feature show that the absence of the 3.1 μm feature in stars with $[K - L] \gtrsim 4$ is expected, because dust emission fills in the feature, if the temperature of the dust at the inner radius is ~ 1500 K, equal to the typical condensation temperature of carbon-rich dust. The presence of a strong 3.1 μm feature in stars with $[K - L] \approx 5$ can be explained if the dust temperature at the inner radius is $\lesssim 700$ K. An alternative explanation is that in those stars there may be a circumstellar contribution to the 3.1 μm feature.

Key words: stars: carbon – circumstellar matter – stars: mass loss – stars: AGB – infrared: stars

1. Introduction

Before the advent of infrared astronomy, the identification of M-, S- and C-stars was based exclusively on optical spectra: M-stars show TiO bands, S-stars display ZrO and LaO bands and carbon stars are easily recognised by the presence of C₂ bands. With the large infrared surveys of the past decades (IRC, AFGL,

IRAS) it has become clear that there are many AGB stars which are so obscured by circumstellar shells that they are weak or invisible in the optical. For these objects, the traditional way to discriminate between different types of AGB stars must be replaced by a method or methods based on the infrared properties of AGB stars.

The infrared dust emission features between 9 and 20 μm have been used as such a tool since their discovery in the late sixties and early seventies. With the publication of the LRS atlas (JISWG 1986, see also Volk & Cohen 1989; Volk et al. 1991) the LRS spectrum has become the most important tool in the infrared for discriminating between carbon stars and oxygen-rich stars. The silicate features at 9.7 and 18 μm are indications for an oxygen-rich star; the silicon carbide (SiC) feature at 11.3 μm is an indication for a carbon-rich star. However, this method is not 100% reliable. The chemistry in the circumstellar shell need not reflect the C/O ratio in the stellar photosphere. There are (optically) known carbon stars which display the silicate feature (Little-Marenin 1986; Willems & de Jong 1986) and known M-stars which apparently are surrounded by carbon-rich shells (Skinner et al. 1990). Moreover, there are many AGB stars which do not exhibit any of the above features clearly in their LRS spectra.

Another method which has been used to infer the carbon or oxygen-rich nature of stars is based on the molecular emission lines in the circumstellar shell. Characteristic of an oxygen-rich star are H₂O, OH and SiO maser emission, while strong HCN emission relative to CO is characteristic for a carbon-rich star. A disadvantage of this method is that (again) it samples the envelope chemistry and not the stellar abundances. Furthermore, definitive statements about the chemistry, based on molecular emission only, are difficult to make. The detection rate of OH maser emission in oxygen-rich AGB stars is 40% at best (te Lintel Hekkert et al. 1991) and oxygen-rich stars also have been detected in HCN (Lindqvist et al. 1988, 1992; Necessian et al. 1989).

A promising diagnostic for distinguishing carbon-rich from oxygen-rich objects is the photospheric 3.1 μm feature observed in carbon stars. This feature is probably due to HCN and C₂H₂

Send offprint requests to: M. Groenewegen at IAP address

* Based on observations obtained at the European Southern Observatory, La Silla, Chile and the UKIRT, Hawaii, U.S.A.. The United Kingdom Infrared Telescope is operated by the Royal Observatory Edinburgh on behalf of the U.K. Science and Engineering Research Council.

Table 1. The program stars

Star	IRAS-name	$[K - L]$	$[12 - 25]$	LRS	3 μm feature	remark
1	02345+5422	5.04	1.35	23	yes	
2	07336-1006	2.98	0.71	15	yes	
3	08074-3615	5.28	1.08	22	yes	
4	11318-7256	1.97	0.33	44	yes	AFGL 4133
5	12419-6058	5.30	1.35	21	no	
6	13045-6404	4.28	1.03	13	yes	
7	13477-6532	4.37	0.98	04	yes	AFGL 4183
8	15194-5115	3.44	0.58	04	yes	
9	17297+1747	2.4	1.22	14	no	IRC 20326, AFGL 1977
10	18464-0656	5.5 ^a	1.49	21	no	AFGL 2256
11	19548+3035	3.6	1.97	21	no	AFGL 2477
12	19558+3333	5.0 ^a	1.63	31	no	
13	19594+4047	3.2	1.27	42	yes	AFGL 2494
14	21318+5631	6.6 ^a	1.47	21	yes	AFGL 5625S
15	21377+5042	2.6 ^a	0.74	15	yes	
16	23166+1655	6.2	1.47	02	yes	AFGL 3068

Note: ^a $K - L$ color based on the blackbody temperature in the 2-4 μm region.

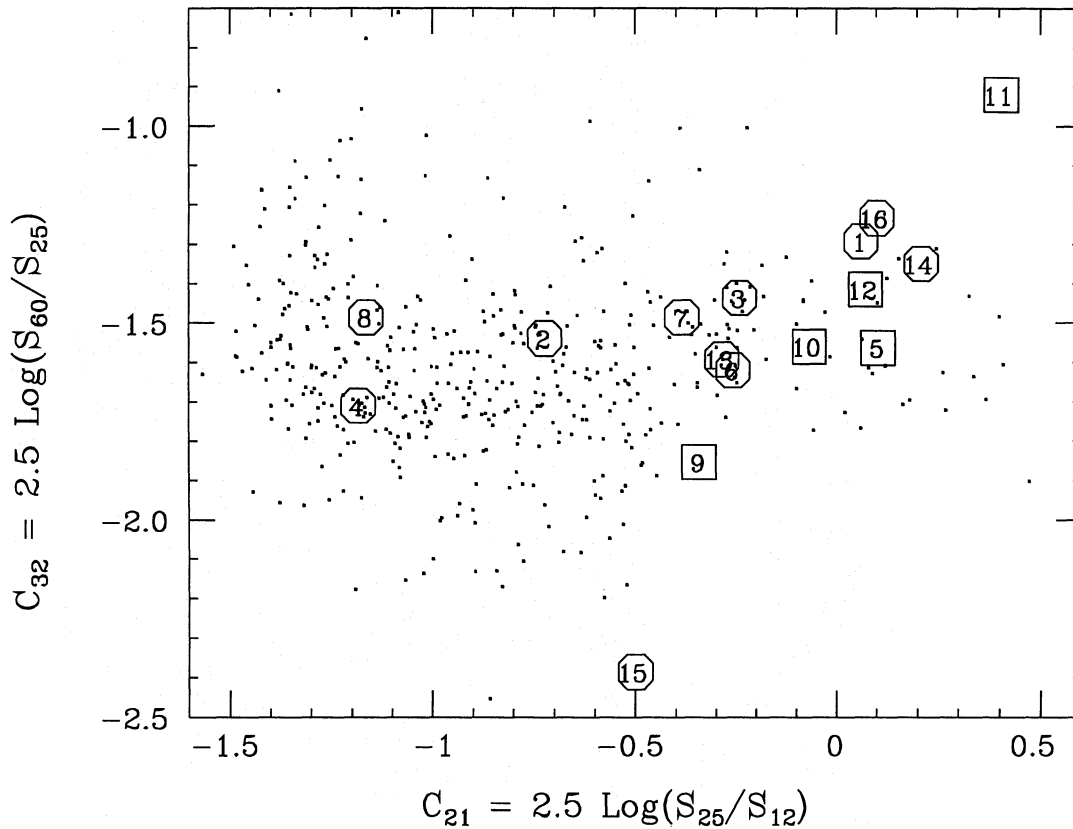


Fig. 1. The IRAS color-color diagram. The program stars are indicated by the running number listed in Table 1. The dots represent all stars from the IRAS Point Source Catalog with LRS = 4n and FQUAL = 3 at all four IRAS bands. Octagons indicate carbon stars with a 3 μm feature and squares indicate stars without a 3 μm feature but with LRS spectra similar to that of carbon stars

(Ridgway et al. 1978) and is observed in optical carbon stars (Noguchi et al. 1977; Merrill & Stein 1976a), in 2 μm bright IRC sources (Merrill & Stein 1976b; Witteborn et al. 1980; Noguchi et al. 1981) and in obscured carbon stars (Merrill & Stein 1976c; Gehrz et al. 1978; Jones et al. 1978). The 3.1 μm feature is not observed in M- and S-stars (Noguchi et al. 1977, 1981, 1993). Advantages of this method are (1) the 3.1 μm feature is either photospheric or formed in circumstellar material very close to the star, rather than in more distant circumstellar gas, and (2) the photospheres of many visually obscured stars are still detectable in the L -band. A disadvantage is that the feature may be filled in due to dust emission¹. Another concern is the possible confusion with the ice feature observed in some cold oxygen-rich objects (e.g. OH/IR stars), which is located at approximately the same wavelength. However, the shape of the ice feature and the feature observed in carbon stars are different (Merrill & Stein 1976a; Noguchi et al. 1977). Furthermore, in most cases an oxygen-rich object can be identified readily from its LRS spectrum, if available.

In this paper we report on 2-4 μm observations of a sample of highly reddened candidate carbon stars. In Sect. 2 the sample is presented and in Sect. 3 the observational procedure is outlined. Section 4 contains discussions of individual stars and groups of stars in the sample. Theoretical modelling of the 3.1 μm feature is presented in Sect. 5 and we conclude in Sect. 6.

2. The sample

Sixteen candidate carbon stars were selected based on the shapes of their LRS spectra. They originate from two subgroups: (1) stars with a possible weak SiC feature, most of which were not classified as 4n objects in the LRS atlas, and (2) stars with almost featureless LRS spectra. The latter class is particularly interesting. Studying a complete sample of IRAS bright carbon stars, Groenewegen et al. (1992) noted that with increasing S_{25}/S_{12} -ratio the SiC feature weakens until the LRS spectrum is almost featureless. Some of these stars with “featureless” LRS spectra are known to be carbon-rich (e.g. AFGL 3068, AFGL 190). Groenewegen et al. (1992) identified 7 stars with “featureless” LRS spectra and $S_{12} > 100$ Jy. Additional stars with “featureless” LRS spectra are listed in Volk et al. (1992) and Omont et al. (1993).

All stars observed are listed in Table 1. The positions of the stars in the IRAS color-color diagram are indicated in Fig. 1. For comparison this figure also includes all stars from the IRAS Point Source Catalog (JISWG 1986) with FQUAL = 3 at all four IRAS bands and LRS = 4n. However, not all stars classified as 4n are carbon stars. In fact, for $C_{21} = 2.5 \log(S_{25}/S_{12}) \gtrsim -0.10$ most stars are oxygen-rich. In those stars, the silicate feature, weakly in absorption, has been misclassified as SiC emission (see Groenewegen et al. 1992; Omont et al. 1993). In Fig. 2 the

¹ We will refer to the influence of dust on the photospheric 3.1 μm feature as ‘filling in the feature’. More accurately, the effect of dust is twofold, since it both obscures the stellar photosphere and adds an infrared continuum. The latter markedly decreases the equivalent width of a photospheric 3.1 μm features (see Sect. 5).

Table 2. Molecular emission of the program stars

IRAS-name	CO	HCN	OH	H ₂ O	SiO	References
11318	Y	Y	-	-	-	1, 1, -, -, -
15194	Y	-	-	-	-	2, -, -, -, -
07336	Y ^a	N	-	-	-	1, 1, -, -, -
21377	-	-	-	-	-	-, -, -, -, -
13477	Y	Y	N	-	-	1, 1, 3, -, -
13045	N ^b	N	N	-	-	1, 1, 3, -, -
08074	Y	Y	N	N	-	2, 2, 3, 4, -
19594	Y	Y	N	-	-	2, 2, 3, -, -
02345	-	-	N	-	-	-, -, 6, -, -
23166	Y	Y	N	-	N	2, 2, 4, -, 4
21318	Y	Y	N	N	-	2, 2, 4, 4, -
17297	Y	Y	N	N	N	2, 5, 4, 4, 7
12419	Y	N	N	-	-	1, 1, 3, -, -
18464	Y	N	N	-	-	1, 1, 6, -, -
19558	-	-	N	N	-	-, -, 4, 4, -
19548	Y	Y	N	N	-	2, 2, 4, 4, -

Y means detected, N means observed but not detected and - means not observed.

^{a)} Probably detected, but strong interstellar contamination.

^{b)} Very uncertain, probably not detected.

References: (1) Groenewegen & de Jong 1994, (2) Loup et al. 1993, (3) te Lintel Hekkert et al. 1991, (4) Benson et al. 1990, (5) Izumiura 1992, (6) Le Squeren et al. 1992, (7) Lindqvist et al. 1992.

positions of the program stars in the $[K - L]$, $[12 - 25]$ diagram are shown. This color-color diagram can be used to distinguish oxygen-rich from carbon-rich objects (e.g. Epchtein et al. 1987). The K and L magnitudes are taken from this work (Sect. 3), Groenewegen et al. (1993), Hrivnak et al. (1989) and Gezari et al. (1987). In case of no available photometry we estimated $[K - L]$ from the 2-4 μm spectrum.

3. The observations

The northern objects were observed with the UKIRT 3.8m telescope on the night of September 7, 1990. The seven-channel cooled grating spectrometer CGS2 was used with an aperture of 5". Standard chopping and nodding techniques were used. The spectral ranges 2.2-2.5, 2.8-3.8 μm were observed with a resolution of 0.008 μm , giving a resolving power $\lambda/\Delta\lambda$ ranging from 300 to 450. All spectra were sampled every 1/2 resolution element and were Hanning-smoothed during data reduction. For IRAS 02345+5422 we obtained near-infrared photometry at the end of the night using the UKT 9 photometer; the results are: $H = 15.8 \pm 0.5$, $K = 11.32 \pm 0.01$, $L = 6.28 \pm 0.01$, $L' = 5.63 \pm 0.01$ and $M = 4.03 \pm 0.01$ magnitudes.

The southern objects were observed with the ESO/MPI 2.2m telescope on February 25-28, 1991. A Circular Variable Filter wheel (CVF) was used in the range 2.9-3.5 μm with $\Delta\lambda = 0.027$, resulting in a resolving power of 110 at 3.1 μm . An aperture of 8" and a throw of 15" were used. The spectra of IRAS 08074, 11318 and 13477 have been published previously

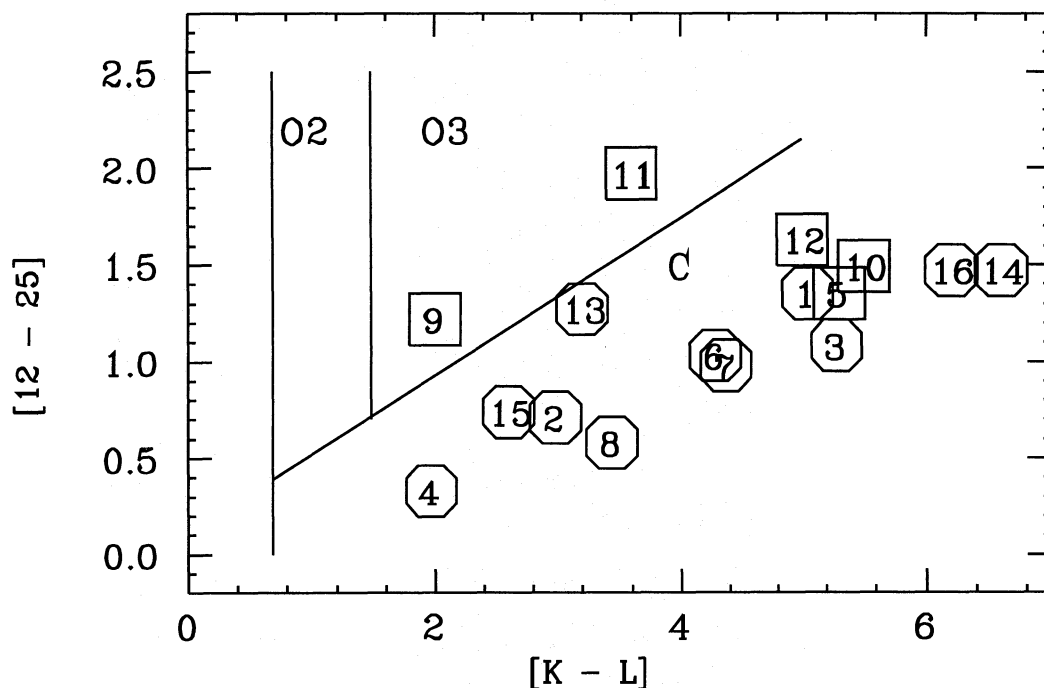


Fig. 2. The $[K - L]$, $[12 - 25]$ color-color diagram. The program stars are indicated by the running number listed in Table 1. The areas marked O2 and O3 are predominantly occupied by oxygen-rich stars, the area marked C by carbon stars (boundaries taken from Epchtein et al. 1987; for the extension of the C area beyond $[K - L] = 3.4$ see Groenewegen et al. 1993). Octagons indicate carbon stars with a 3 μm feature and squares indicate stars without a 3 μm feature but with a LRS spectrum similar to that of carbon stars. The location of sources '9' and '11' is discussed in Sect. 4.2

by Groenewegen & de Jong (1991). For most southern sources *JHKLM* photometry is available (Groenewegen et al. 1993).

During both observing runs we peaked up on the infrared sources in the *L*-band. The position observed was always in good agreement with the IRAS position or other infrared positions listed in the literature. We used the standard reduction technique of dividing the source spectrum by the (featureless) standard star spectrum observed at the same airmass as the program star and then multiplying either by the assumed blackbody temperature of the standard star or the known continuum flux in the case of G-dwarfs (Koornneef 1983, only for the ESO observations). This provides adequate cancellation of atmospheric features, except near 3.32 μm where in the UKIRT spectra a residual telluric feature may still be seen. Absolute calibration was achieved by adopting a *K* or *L* magnitude for the standard star. The statistical uncertainty in the fluxes is less than 5%.

4. The results

In this section the observed 2-4 μm spectra are discussed. The stars are divided into two groups: (1) stars which show the 3 μm feature and therefore are carbon stars, and (2) stars which do not. We searched the literature for observations of CO, HCN, OH, H₂O and SiO molecular emission to help discriminate between carbon- and oxygen-rich objects. The results are collected in Table 2.

4.1. The stars with the 3.1 μm feature

In Fig. 3 the LRS spectra and the 2-4 μm spectra are presented in order of increasing $[12 - 25]$ color. All stars in the figure show a 3 μm feature and are therefore carbon stars. The observations show that the feature is located between 2.9 and 3.2 μm . A residual feature at 3.32 μm is due to incomplete cancellation of the strong telluric CH₄ Q-branch absorption bands. In Fig. 4, in order to make the weak features in two of the stars (IRAS 23166, IRAS 21318) more apparent we have divided their 2-4 μm spectra by "continua," determined by fitting blackbody curves to their spectra outside the feature,

In several of the high-resolution UKIRT observations two sub-features can be identified, one with a minimum near 3.02 μm and the other with a minimum near 3.10 μm . The differences in the overall shape and in the relative strengths of the two sub-features probably can be ascribed at least partially to differences in the excitation of the relevant molecules, as the 3.1 μm feature as a whole is a blend of vibrational-rotational transitions of HCN and C₂H₂.

Four of the stars in this group were already known to be carbon stars. The object with the bluest colors and the strongest SiC feature, IRAS 11318, is number 3062 in Stephenson's catalog (1989) of (optical) carbon stars². IRAS 15194, 19594, and 23166 have published 2-4 μm spectra (Meadows et al. 1987;

² IRAS 13477 and 15194 are also listed in Stephenson's catalog under number 3439 and 3592, respectively. These two stars were included

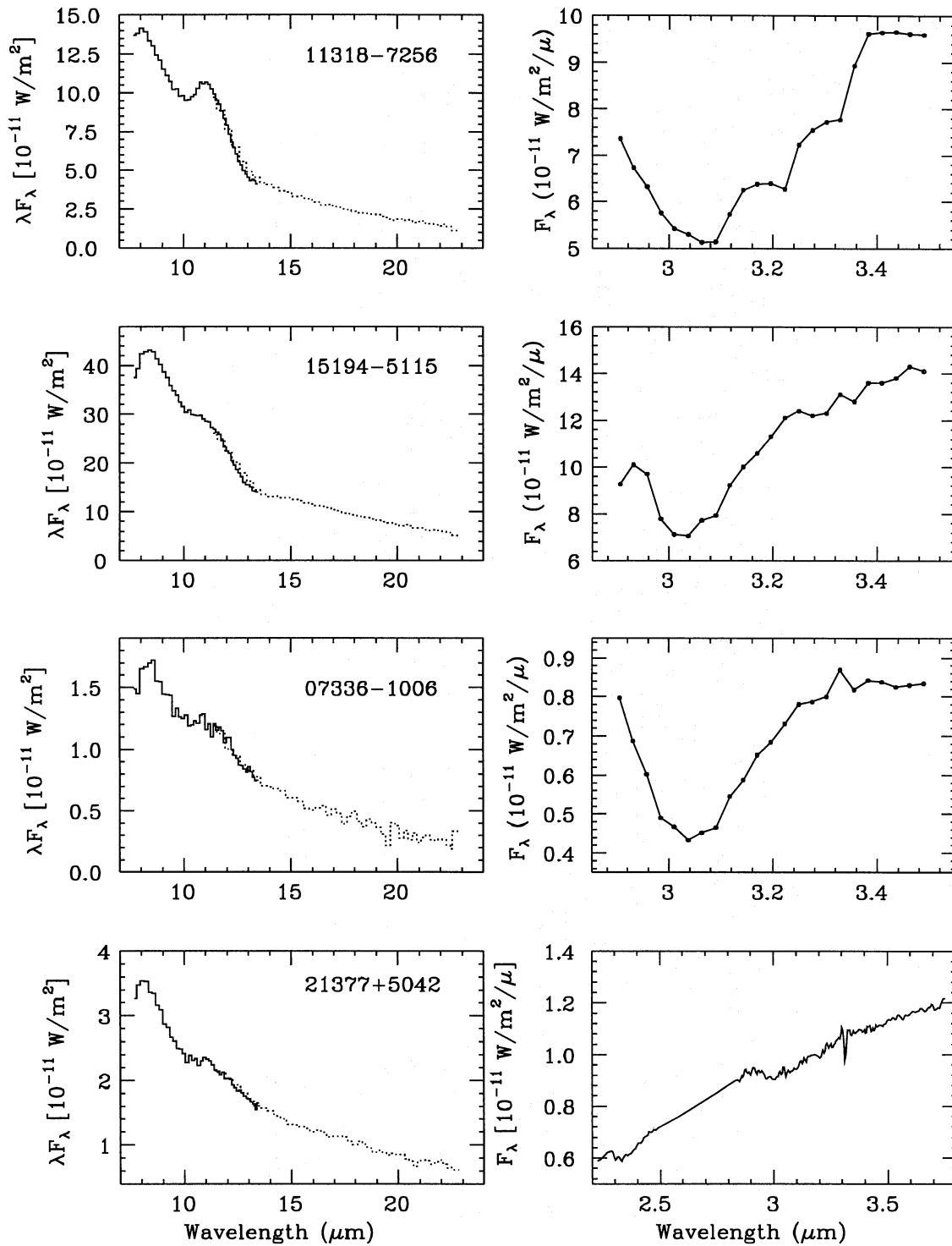


Fig. 3. The LRS spectra (left-hand panel) and 2-4 μm spectra (right-hand panel) for the carbon stars

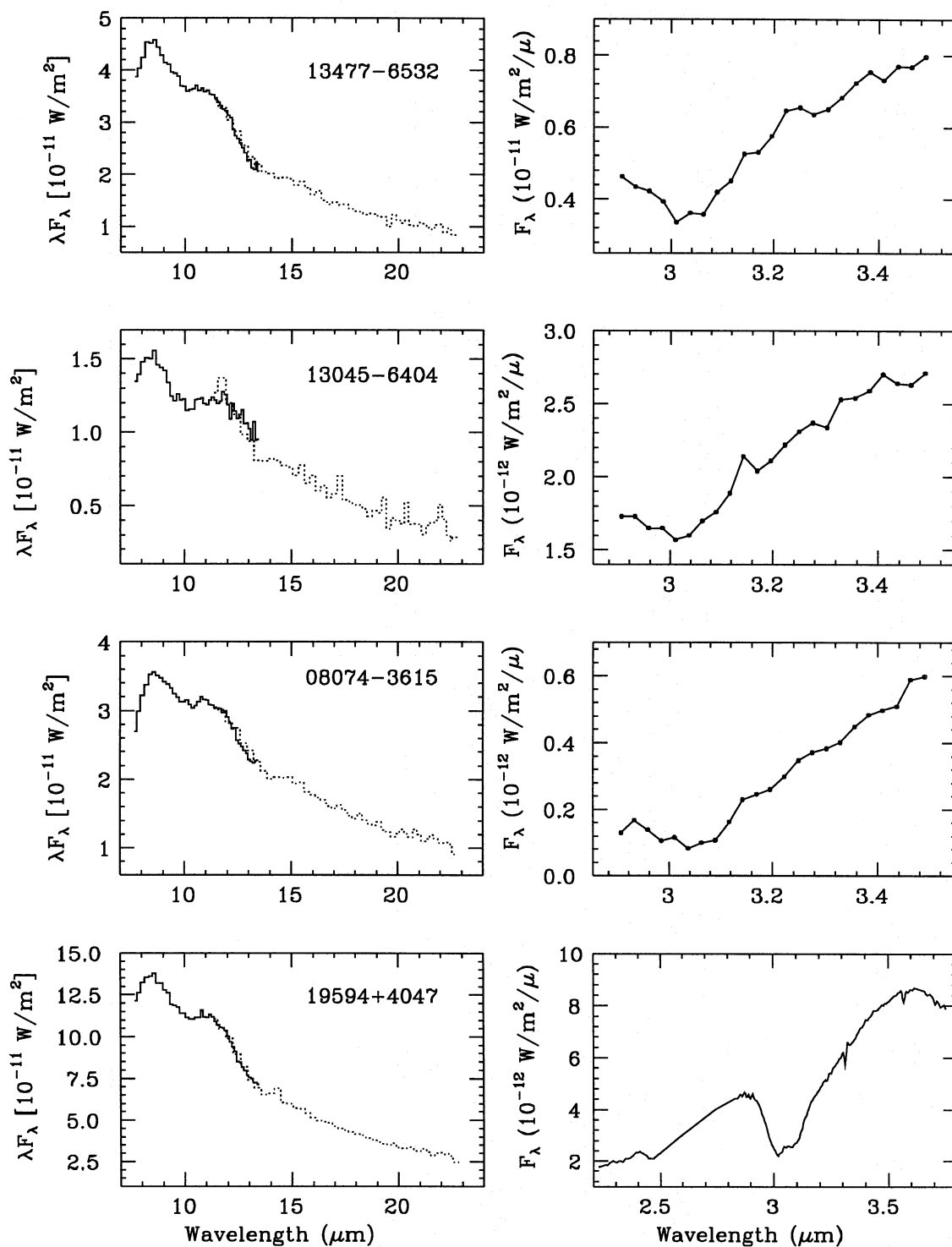


Fig. 3. (continued)

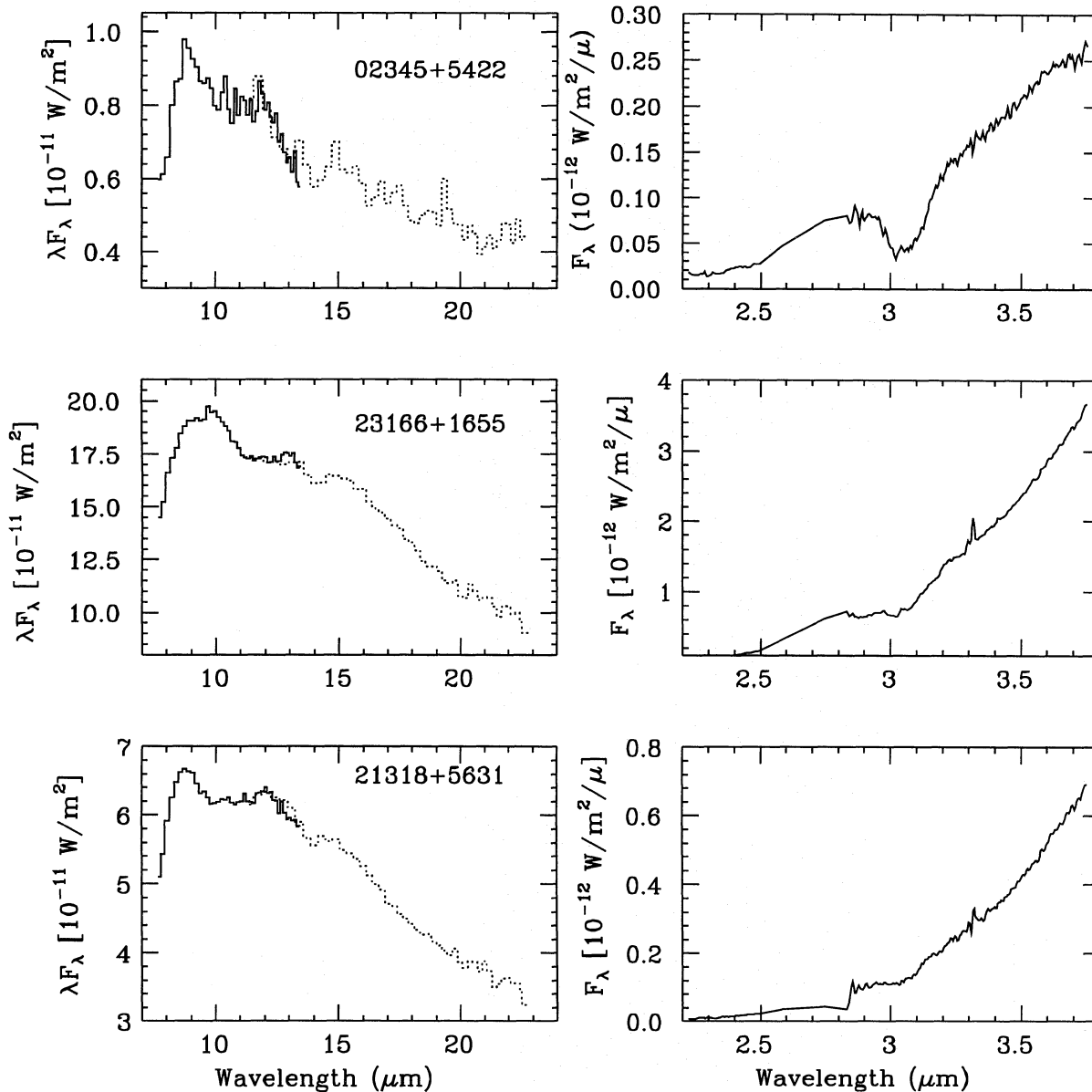


Fig. 3. (continued)

Merrill & Stein 1976c; Jones et al. 1978) which show the 3.1 μm feature; they were included as reference objects for the ESO and UKIRT observations.

4.2. Possible carbon stars without the 3.1 μm feature

In Fig. 5 the LRS and 2-4 μm spectra are shown of the five objects without detectable 3 μm feature but with LRS spectra similar to those of known carbon stars. The 2-4 μm spectra are divided by the continuum (except for IRAS 19548), which was determined as described above. The objects in this group are discussed individually, in order of increasing [12 - 25] color.

in Stephenson's catalog on the basis of the presence of the SiC feature (Little-Marenin et al. 1987) and not on the basis of an optical spectrum.

17297+1747

The LRS spectrum of this peculiar object is similar to that of IRAS 07336. The star is located in region O3 of the $[K - L]$, [12 - 25] diagram. Omont et al. (1993) classify it as 'O?'. In the compilation of Bidelman (1980) this star (IRC 20 326) is listed as a bright ($V = 9.6$) variable star with spectral classification 'M2, blend with?'. Based on the appearance of its 2 μm spectrum Frogel et al. (1975) classify it as a carbon star. The star is not detected in OH, H₂O and SiO but is detected in HCN (Table 2).

The HCN/CO(1-0) ratio can be used to discriminate between oxygen- and carbon-rich objects (Bujarrabal et al. 1994). The HCN velocity integrated intensity measured at the Nobeyama telescope is 2.0 K kms^{-1} (Izumiura 1991). From Loup et al.

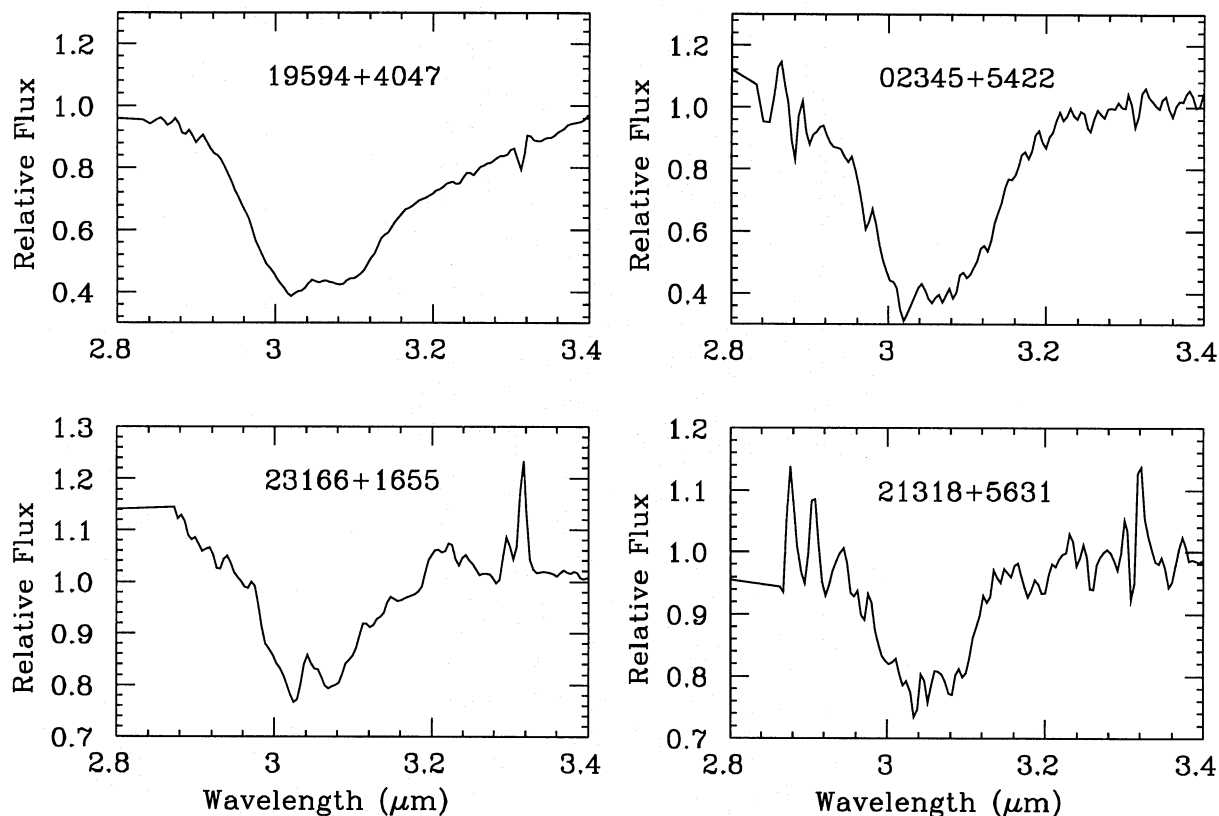


Fig. 4. The shape of the 3.1 μm feature

(1993), CO(1-0) velocity integrated intensities are available from the BTL, OSO and FCRAO telescopes. From stars in common between Loup et al. (1993) and Izumiura (1991) for which he did observe CO(1-0) we derive conversion factors of $\text{Nob/BTL}=3.6 \pm 0.6$ ($N=14$), $\text{Nob/OSO}=0.91 \pm 0.25$ ($N=12$), $\text{Nob/FCRAO}=1.3 \pm 0.2$ ($N=7$). Scaling the CO observations to the Nobeyama telescope than gives predicted intensities of 19.2 ± 3.2 (BTL), 18.1 ± 2.5 (FCRAO) and 18.9 ± 5 (OSO) K km s^{-1} . The ratio $\text{HCN/CO}(1-0)$ is therefore about 0.11, below the mean value observed in carbon stars (0.52; Bujarrabal et al. 1994), but not low enough to exclude a carbon star nature. Modelling of the 2-4 μm region may suggest this star is not a carbon star (Sect.5, Fig. 6)

12419–6058

This is the reddest star we observed at ESO, at relative low resolution. The scatter of data points in the 3.0-3.2 μm region is due to noise. We cannot exclude the possibility that at higher signal-to-noise a weak 3.1 μm feature may be present. The LRS spectrum is similar to that of IRAS 08074. The star is located in region C of the $[K-L]$, $[12-25]$ diagram.

18464–0656

The LRS spectrum is similar to the carbon star IRAS 08074. The star is located in region C of the $[K-L]$, $[12-25]$ diagram. The star is detected in CO but not in HCN and OH. Omont et

al. (1993) classify it as carbon-rich. The broad depression in the 2-4 μm spectrum probably is an artifact of fitting the continuum with a single blackbody temperature.

19558+3333

The LRS spectrum is similar to that of IRAS 02345. The star is located in region C of the $[K-L]$, $[12-25]$ diagram. The star is not detected in OH and H_2O , consistent with a carbon-rich nature. Omont et al. (1993) classify it as oxygen-rich, Kwok et al. (1987) suggest it to be a carbon star.

19548+3035

The LRS spectrum of this object is similar to that of IRAS 21318. The star is located in region O3 in the $[K-L]$, $[12-25]$ diagram. The star is detected in HCN and the velocity integrated ratio $\text{HCN/CO}(1-0)$ is 0.24 (from Loup et al. 1993), marginally larger than the value of 0.18 suggested by Bujarrabal et al. (1994) to separate carbon from oxygen-rich stars. The star is not detected in OH and H_2O , suggesting a carbon-rich nature. Kwok et al. (1987) suggest it to be a carbon star.

The 2-4 μm spectrum (Fig. 5b) suggests that IRAS 19548 is a post-AGB star in which central star dominates at $\lambda < 2.6 \mu\text{m}$ and a detached shell dominates at $\lambda > 3 \mu\text{m}$. A post-AGB evolutionary status of this object was recently suggested by Volk

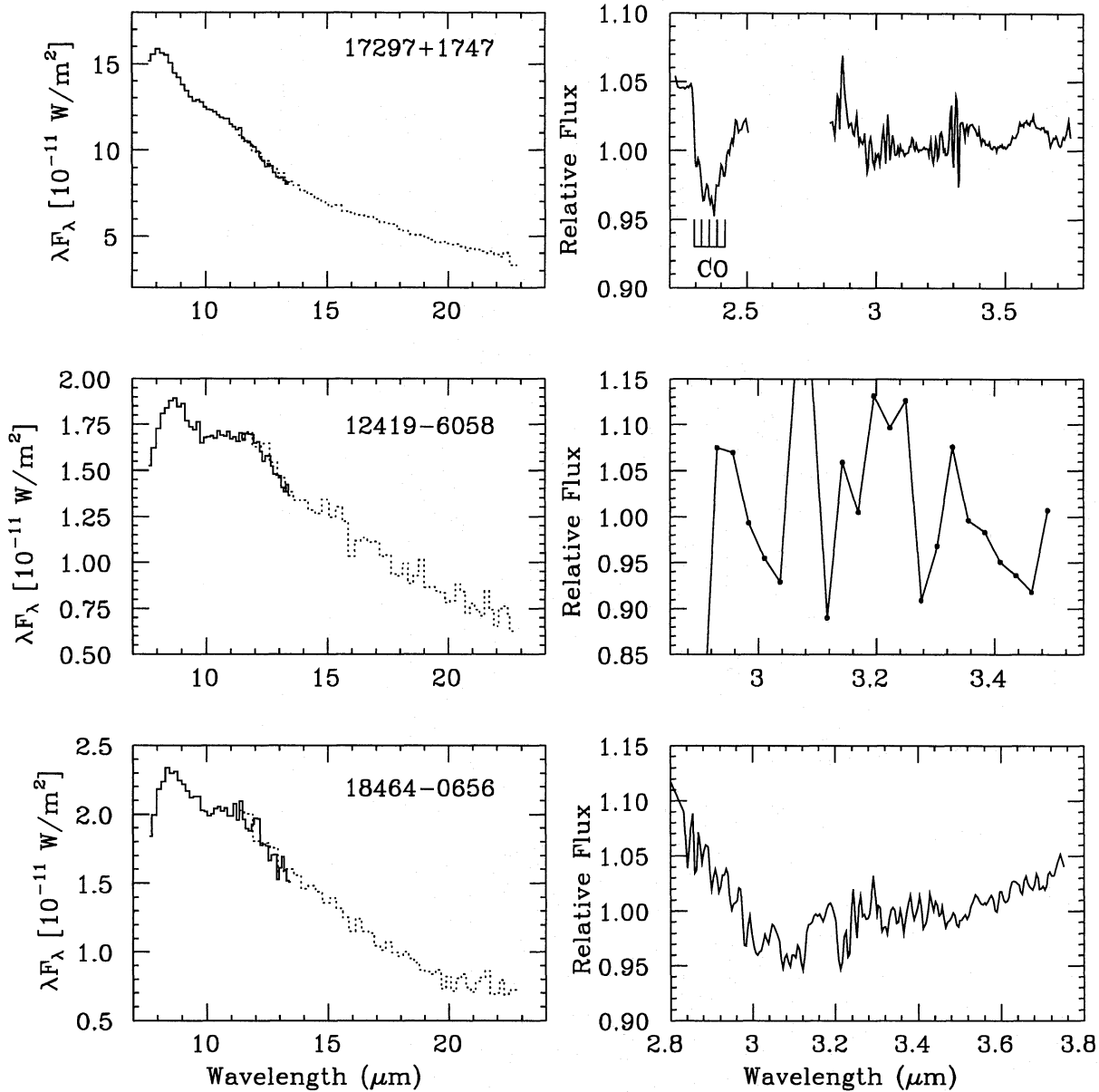


Fig. 5. The LRS spectra (left-hand scale) and 2-4 μm spectra (divided by the continuum; right-hand scale) for the stars without a detectable 3 μm feature but with LRS spectra very similar to the carbon stars. All are UKIRT/CGS2 spectra except for IRAS 12419. The positions of the CO band heads are indicated for IRAS 17297

et al. (1992) based on the shape of the spectral energy distribution. The bandheads of the CO ($v = 2-0$ to $v = 7-5$) transitions are identified near 2.3 μm . The presence of strong CO absorption indicates that the temperature of the stellar photosphere is 4000 K or less.

The shape of the SED in the 2-4 μm region explains the relative blue $[K - L]$ color of this star. Extrapolating the emission of the dust shell (at $\lambda \gtrsim 3.2 \mu\text{m}$) to 2.2 μm results in an $[K - L]$ color of the dust shell of about 5.4. This would move the star from region O3 to C in the $[K - L]$, $[12 - 25]$ diagram (Fig. 2).

5. Theoretical modelling of the 3.1 μm feature

In Fig. 6 we plot the strength of the feature (defined as the natural logarithm of the ratio of the interpolated continuum flux at 3.1 μm to the flux at 3.1 μm ; denoted Y) against $[K - L]$ color for the 16 stars we observed. To interpret the distribution of the observations in Fig. 6, consider the following simple model.

The flux, F_λ , observed at Earth at a distance d from a central star surrounded by a circumstellar dust shell may be approximated as:

$$d^2 F_\lambda = R_*^2 \pi B_\lambda(T_{\text{eff}}) \exp(-\tau_\lambda^{\text{dust}}) \exp(-\tau_\lambda^{\text{feature}}) + R_{\text{dust}}^2 \pi B_\lambda(T_{\text{dust}}) (1 - \exp(-\tau_\lambda^{\text{dust}})), \quad (1)$$

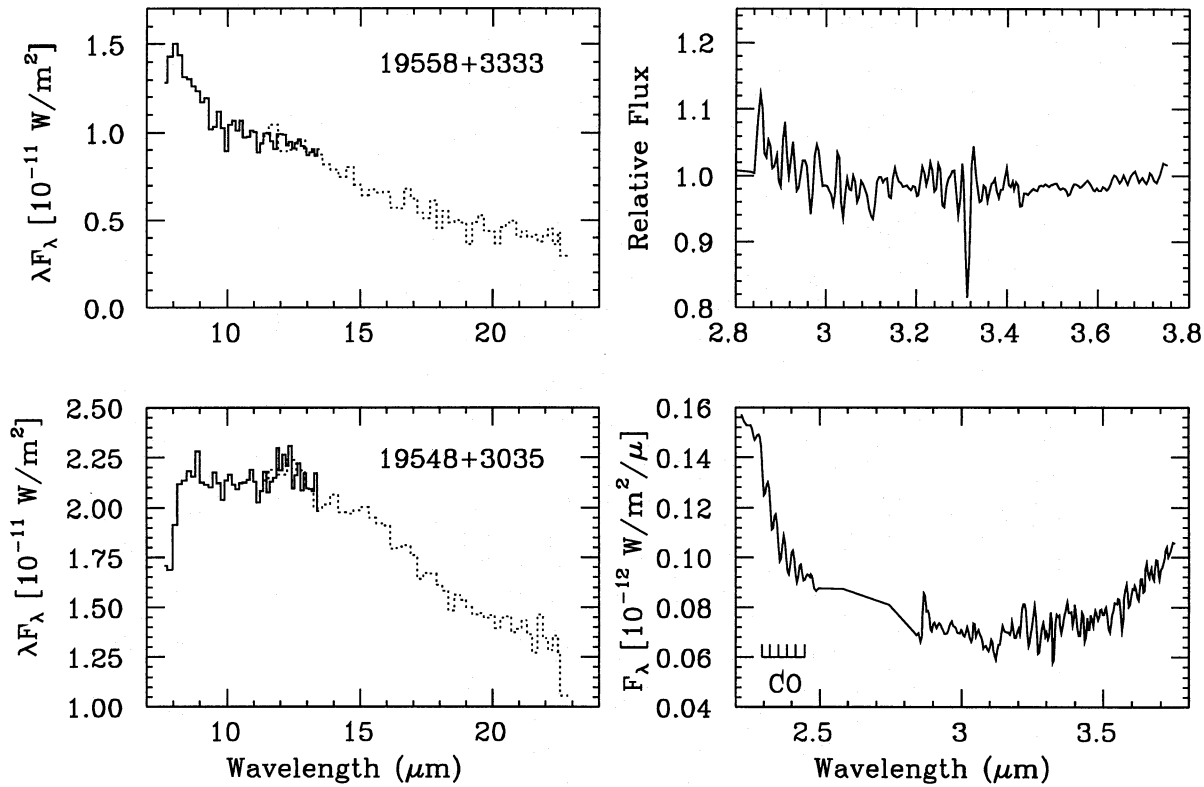


Fig. 5. (continued) For IRAS 19548 band heads of the CO vibrational $\Delta v = 2$ transitions are indicated

where R_* is the stellar radius. The optical depth near 3 μm can be written as:

$$\tau_{\lambda}^{\text{feature}} = A e^{-\left(\frac{\lambda - \lambda_0}{\Delta\lambda}\right)^2}, \quad (2)$$

where A is the strength of the feature, $\lambda_0 = 3.1 \mu\text{m}$, and $\Delta\lambda$ is related to the width of the feature. The dust optical depth ($\tau_{\lambda}^{\text{dust}}$) scales linearly with the mass loss rate. In Eq. (1) one should use the inner dust radius and the dust temperature at the inner dust radius (i.e. the condensation temperature T_c of the dust) for R_{dust} and T_{dust} , respectively, if $\tau_{\lambda}^{\text{dust}} < 1$. If $\tau_{\lambda}^{\text{dust}} > 1$ then one should use the radius (and the dust temperature at that radius) where $\tau_{\lambda}^{\text{dust}} = 1$.

If there is no mass loss then $Y = A$, and $[K - L]$ is determined by the value of T_{eff} . If the mass loss increases (for a fixed value for T_{dust}) then $[K - L]$ increases, since the spectrum is more and more determined by T_{dust} instead of T_{eff} . The value of Y decreases due to extinction effects and the increasing importance of the dust continuum (see Eq. 1). The effect of lowering the dust temperature at the inner radius (for fixed $\tau_{\lambda}^{\text{dust}}$) is to increase the strength of the feature: the dust emission becomes less since $B_{\lambda}(T_1) < B_{\lambda}(T_2)$ for all λ , if $T_1 < T_2$.

Although the simple model contains all essential physics we use the dust radiative transfer model of Groenewegen (1993) to quantitatively model the relation between Y and $[K - L]$. In the model the radiative transfer and radiative equilibrium equation for the dust are solved simultaneously in spherical geometry. For the dust properties we assume amorphous carbon grains (optical

constants listed in Rouleau & Martin 1991) of radius $a = 0.05 \mu\text{m}$ and specific density $\rho_d = 2.0 \text{ gr cm}^{-3}$. Typical parameters of $T_{\text{eff}} = 2500 \text{ K}$, a dust-to-gas ratio of $\Psi = 0.01$, and an outflow velocity of $v = 15 \text{ km s}^{-1}$ are assumed. We consider a feature of strength $A = 4.605$, corresponding to a 99% depression at λ_0 in the central star. This maximizes the contribution of the 3.1 μm feature in the central star relative to the dust contribution. For T_c we consider 1500 K, the usual value for the carbon dust condensation temperature, $T_c = 700 \text{ K}$, and $T_c = 500 \text{ K}$. The results are shown in Fig. 6.

The fact that the models do not predict $[K - L] \lesssim 3$ is an artifact of using a blackbody representation of $T_{\text{eff}} = 2500 \text{ K}$ for the spectrum of the central star, which dominates the $[K - L]$ color for low mass loss rates. The calculations show that dust emission is important in decreasing the strength of the feature for $\dot{M} \gtrsim 10^{-6} - 10^{-5} M_{\odot}/\text{yr}$, depending on T_c . For $[K - L] \lesssim 4$ we expect to detect a 3.1 μm feature in any star that is a carbon star. IRAS 17297 and IRAS 19548 have such colors and do not have an 3.1 μm feature. IRAS 19548 was discussed in Sect. 4.2 where it was argued that the color of the dustshell is $[K - L] \approx 5.4$ (see Fig. 5b). The location of IRAS 17297 in Fig. 6 suggests either an unusually low intrinsic photospheric absorption strength of the 3.1 μm feature, or the star is not a carbon star.

Although one might have expected to see a decrease in feature strength with increasing $[K - L]$, no obvious trend is evident in the observed data. Indeed, the two objects with the strongest 3.1 μm features have $[K - L]$ near 5. The lack of a trend may be due to the small number of data points coupled with differ-

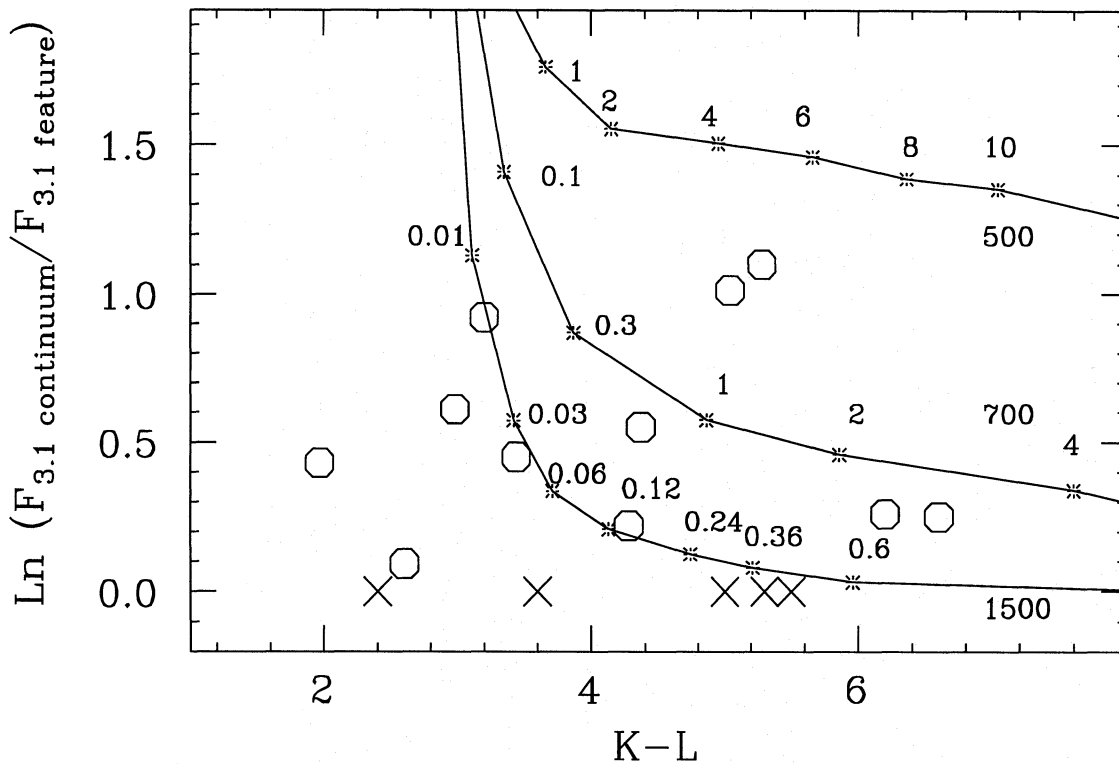


Fig. 6. Theoretical modelling of the 3.1 μm feature. Along the Y-axis the natural logarithm of the ratio of the interpolated continuum flux at 3.1 μm to the flux at 3.1 μm is plotted, along the X-axis the $[K - L]$ magnitude. The stars with (O) and without (X) 3.1 μm feature are indicated. The two X's at $[K - L] = 2.4$ and 3.6 are IRAS 17297 and IRAS 19548, which are discussed in the text. The curves are the result of theoretical modelling as described in the text. The curves are labelled by the temperature of the dust at the inner radius of the circumstellar dust shell, and along each curve the mass loss rate in $10^{-5} M_{\odot}/\text{yr}$ is indicated

ences in intrinsic photospheric absorption strengths from object to object, as well as differences in dust temperature. The two stars with the strongest absorptions can only be explained if the dust is much cooler than the condensation temperature of 1500 K and, hence, that their circumstellar shells are well detached from the central stars.

Interpretation of the data is further complicated by the possibility that the 3.1 μm feature may not be entirely photospheric, and originate in part in the circumstellar shell. In the previous calculation we assumed that the 3.1 μm feature is formed in the photosphere. Ridgway et al. (1978) derive from their high-resolution spectra of the 3.1 μm feature in IRC 10 216 a rotational temperature of 400-800 K, consistent with absorption in the circumstellar shell. To investigate this possibility for the present sample would require observations at a much higher resolution to resolve the rotational lines and determine their excitation temperature.

6. Conclusions

We have searched a sample of 16 candidate carbon stars for the 3.1 μm absorption feature. We confirm 11 of these as carbon stars, on the basis of detection of this feature. Five stars do not show the 3.1 μm feature. However, the LRS spectra, the

molecular emission signatures and/or the location in the $[K - L]$, $[12 - 25]$ color-color diagram suggest in at least four cases that these are carbon stars.

Although one would predict that the strength of the 3.1 μm feature would decrease with increasing $[K - L]$, no trend is evident. Observations of additional obscured carbon star candidates are needed in order to improve the statistics. Two stars with large $[K - L]$ have unusually strong 3.1 μm features. Based on a theoretical model we show that the dust temperature at the inner radius of the circumstellar dust shell may be as low as 600 K in those cases.

Acknowledgements. The research of MG was supported under grant 782-373-030 by the Netherlands Foundation for Research in Astronomy (ASTRON), which is financially supported by the Netherlands Organisation for Scientific Research (NWO). We thank Rens Waters for his comments on the manuscript.

References

- Benson P.J., et al., 1990, ApJS 74, 911
- Bidelman W.P., 1980, Publ. Warner and Swasey Obs., Vol. 2, 185
- Bujarrabal V., Fuente A., Omont A., 1994, ApJL, submitted
- Epchtein N., et al., 1987, A&AS 71, 39
- Frogel J.A., Dickinson D.F., Hyland A.R., 1975, ApJ 201, 392

- Gehrz R.D., Hackwell J.A., Briotta A., 1978 ApJ 221, L23
Gezari D.Y., Schmitz M., Mead J.M., 1987, Catalog of Infrared Observations, NASA reference publication 1196
Groenewegen M.A.T., de Jong T., 1991, The ESO Messenger 66, 40
Groenewegen M.A.T., de Jong T., van der Blik N.S., Slijkhuis S., Willems F.J., 1992, A&A 253, 150
Groenewegen M.A.T., de Jong T., Baas F., 1993, A&AS 101, 513
Groenewegen M.A.T., 1993, Chapter 5, Ph.D. thesis, University of Amsterdam
Groenewegen M.A.T., de Jong T., 1994, A&A, in preparation
Hrivnak B.J., Kwok S., Volk K.M., 1989, ApJ 346, 265
Izumiura H., 1991, Ph. D. thesis, University of Tokyo
Joint IRAS Science Working Group, 1986, IRAS catalogs and atlases, Low Resolution Spectrograph (LRS), A&AS 65, 607
Joint IRAS Science Working Group, 1986, IRAS catalogs and atlases, Point Source Catalog (PSC), US Government Printing Office, Washington
Jones B., Merrill K.M., Puetter R.C., Willner S.P., 1978, AJ 83, 1437
Koornneef J., 1983, A&A 128, 84
Kwok S., Hrivnak B.J., Boreiko R.T., 1987, ApJ 312, 303
Le Squeren A.M., Sivagnanam P., Denneveld M., David P., 1992, A&A 254, 133
Little-Marenin I.R., 1986, ApJ 307, L15
Little-Marenin I.R., Ramsey M.E., Stephenson C.B., Little S.J., Price S.D., 1987, AJ 93, 663
Lindqvist M., Nyman L.-A., Olofsson H., Winnberg A., 1988, A&A 205, L15
Lindqvist M., Olofsson H., Winnberg A., Nyman L.-A., 1992, A&A 263, 183
te Lintel Hekkert P., Caswell J.L., Habing H.J., Haynes R.F., Norris R.P., 1991, A&AS 90, 327
Loup C., Forveille T., Omont A., Paul J.F., 1993, A&AS 99, 291
Meadows P.J., Good A.R., Wolstencroft R.D., 1987, MNRAS 225, 43P
Merrill K.M., Stein W.A., 1976a, PASP 88, 285
Merrill K.M., Stein W.A., 1976b, PASP 88, 294
Merrill K.M., Stein W.A., 1976c, PASP 88, 874
Nercessian E., Guilleoteau S., Omont A., Benayoun J.J., 1989, A&A 210, 225
Noguchi K., Kaware K., Kabayashi Y., Okuda H., Sato S., 1981, PASJ 33, 373
Noguchi K., Kobayashi Y., 1993, PASJ 45, 85
Noguchi K., Maihara T., Okuda H., Sato S., 1977, PASJ 29, 511
Omont A., et al., 1993, A&A 267, 515
Ridgway S.T., Carbon D.F., Hall D.N., 1978, ApJ 225, 138
Rouleau F., Martin P.G., 1991, ApJ 377, 526
Skinner C.J., Griffin I., Whitmore B., 1990, MNRAS 243, 78
Stephenson C.B., 1989, Publ. Warner and Swasey Obs., Vol. 3, 55
Volk K., Cohen M., 1989, AJ 98, 931
Volk K., Kwok S., Langill P.P., 1992, ApJ 391, 285
Volk K., Kwok S., Stencel R.E., Brugel E., 1991, ApJS 77, 607
Willems F.J., de Jong T., 1986, ApJ 309, L39
Witteborn F.C., et al., 1980, ApJ 238, 577